2010

Co-localization of Amanitin and a Candidate Toxin-Processing Prolyl Oligopeptidase in Amanita Basidiocarps

Hong Lou
University of Nebraska, Lincoln

Heather E. Hallen-Adams
University of Nebraska at Lincoln, hhallen-adams2@unl.edu

John S. Scott-Craig
Michigan State University

Jonathan D. Walton
Michigan State University

EC Accepts, published online ahead of print on 1 October 2010
Eukaryotic Cell doi:10.1128/EC.00161-10

September 9, 2010

Co-localization of Amanitin and a Candidate Toxin-Processing Prolyl Oligopeptidase in *Amanita* Basidiocarps

Hong Luo, Heather E. Hallen-Adams[1], John S. Scott-Craig, and Jonathan D. Walton*

Department of Energy Plant Research Laboratory, Michigan State University, E. Lansing MI 48824

[1]Current address: Department of Food Science and Technology, 319 Food Industry Complex, University of Nebraska, Lincoln, NE 68583

* Corresponding author. Mailing address: Department of Energy Plant Research Laboratory, Michigan State University, E. Lansing MI 48824. Phone: (1) 517 353 4885. Fax: (1) 517 353 9168. E-mail: walton@msu.edu

Fungi in the basidiomycetous genus *Amanita* owe their high mammalian toxicity to the bicyclic octapeptide amatoxins such as α-amanitin. Amatoxins and the related phallotoxins (such as the heptapeptide phalloidin) are encoded by members of the "MSDIN" gene family and synthesized on ribosomes as short (34 - 35 amino acid) proproteins. Anti-amanitin antibodies and confocal microscopy were used to determine the cellular and subcellular localization of amanitin accumulation in basidiocarps (mushrooms) of the Eastern North American destroying angel (*Amanita bisporigera*). Consistent with previous studies, amanitin is present throughout the basidiocarp (stipe, pileus, lamellae, trama, and universal veil), but it is present in only a subset of cells within these tissues. Restriction of amanitin to certain cells is especially marked in the hymenium. Several lines of evidence implicate a specific prolyl oligopeptidase, AbPOPB, in the initial processing of the amanitin and phallotoxin proproteins. The gene for AbPOPB is restricted taxonomically to the amatoxin-producing species of *Amanita* and is clustered in the genome with at least one expressed member of the MSDIN gene family. Immunologically, amanitin and AbPOPB show a high degree of co-localization, indicating that toxin biosynthesis and accumulation occur in the same cells and possibly in the same sub-cellular compartments.

More than 90% of all fatal mushroom poisonings are due to species of *Amanita* in section *Phalloideae* such as the death cap (*A. phalloides*), and the destroying angel species complex (*A. bisporigera*, *A. verna*, *A. virosa*, and *A. ocreata*) (3). The toxic agents are a family of bicyclic octapeptides known as amatoxins, which survive cooking and the human digestive tract and are actively taken up by liver and other cells. The biochemical target of the amatoxins is RNA polymerase II, the major enzyme transcribing protein-coding mRNAs in eukaryotic cells (4). The human LD_{50} for α-amanitin is ~0.1 mg/kg, and one mushroom can contain a fatal dose of 10-12 mg (36). Irreversible liver failure and death may result 3-7 days after ingestion.

The amatoxins (and the chemically related phallotoxins such as phallacidin and phalloidin) are synthesized on ribosomes and not, like all other known fungal cyclic peptides, by nonribosomal peptide synthetases (10, 32). Amatoxins are translated as 35-amino acid proproteins and must undergo several posttranslational modifications, including proteolytic cleavage, cyclization, hydroxylation, and formation of a unique tryptophan-cysteine cross-bridge called tryptathionine (19). The amatoxin and phallotoxin genes are members of a large family, called the “MSDIN” family, that are predicted to encode proproteins of 34 to 37 amino acids with conserved upstream and downstream sequences flanking a hypervariable region of 7 to 10 amino acids. The hypervariable region gives rise to the linear peptides corresponding to the mature toxins (18). Certain species of *Amanita* have thus evolved the genetic potential to synthesize a large variety of small, cyclic peptides using the same fundamental biochemical mechanism.

In the MSDIN family of genes, both the amino acid immediately preceding the toxin region and the last amino acid in the toxin region itself are invariant Pro residues (10). All known amatoxins and phallotoxins, as well as other cyclic peptides that have been identified in *A. phalloides*, contain at least one Pro (36). A peptidase that cleaves a synthetic phalloidin peptide at the carboxy-side of both Pro residues to release the linear phalloidin heptapeptide was purified from the phalloidin-producing mushroom *Conocybe apala* (=*C. lactea* or *C. albipes*) (18). This processing peptidase was identified as a member of the prolyl oligopeptidase (POP) family of proteases (6, 29). Due to limiting amounts of biological material (*Amanita* does not form fruiting bodies in culture), and the instability of the enzyme, it has not yet been possible to determine if a POP enzyme also processes the amanitins in species of *Amanita*.

Temporal and structural sequestration is a common feature of secondary metabolism in micro-organisms and plants, serving to prevent these often biologically active compounds from interfering with primary metabolism and to insure their presence at the ecologically most appropriate time and place (16). Mushrooms (here defined as the basidiocarps of macrofungi in the phylum Basidiomycota) produce a number of biologically active secondary metabolites, and some mechanism of separation from primary metabolism would seem to be essential for both the amatoxins and the phallotoxins, since their sites of action (RNA polymerase II and F-actin, respectively) are present in all eukaryotic cells.

Many secondary metabolites are known to be synthesized in specialized cells in other organisms, such as plant trichomes and cone snail secretory ducts (16, 34). However, little is known about the relationship between chemical and structural cellular

specialization in relation to natural product production in macrofungi. Besides the amatoxins and phallotoxins, examples of biologically active molecules from mushrooms include psilocybin, lovastatin, muscarine, ibotenic acid, muscimol, strobilurins, pleuromutilin, and illudins (1, 27). Specialized mushroom structures known or suspected to contain toxic compounds include cystidia in genera such as *Inocybe*, *Russula*, and *Strobilurus*, which are poisonous to mammals or insects (13, 15, 17, 23). *Conocybe apala*, which makes phalloidin, has specialized secretory cells that are toxic to nematodes (12). *Pleurotus cystidiosus* makes specialized cells (toxocysts) consisting of a liquid droplet containing nematocidal compounds surrounded by an elastic adherent envelope (30). Differential cytological staining indicates that many mushrooms contain biochemically specialized hyphae, called secretory hyphae, that are intermingled with the structural hyphae (5). However, the relationship between structure and chemistry has rarely been established in any mushroom, i.e., whether the active compounds are actually located in the specialized cell types.

In this paper, we use a specific anti-amanitin antibody to localize the sites of amanitin accumulation in relation to the cellular distribution of AbPOPB, an enzyme implicated in the post-translational processing of the amatoxin proproteins. The results indicate that amanitins are synthesized and stored in a subset of cells found throughout the mushrooms.

MATERIALS AND METHODS

Biological material. Mushrooms of the Eastern North American destroying angel (*Amanita bisporigera*) were collected in Ingham County, Michigan, in July and August of

2008 and 2009 (Fig. 1). Very young fruiting bodies (button stage, still enclosed in the universal veil, and not yet emerged above the ground) were also collected when possible (Fig. 1). Mushrooms were fixed in 4% paraformaldehyde within 2 to 4 hr of collection. All the mushrooms used in this study were analyzed by HPLC to confirm the presence of amanitins (7, 11). Amanitin concentrations varied from mushroom to mushroom, and samples with higher concentrations were chosen for the immunohistochemical analyses.

Amatoxin and phallotoxin-lacking species of *Amanita* (*A. citrina* and *A. muscaria*) were also collected in the same location as controls. The other *Amanita* species used as a source of DNA for blotting were previously described (10).

Immunological and microscopic methods. To prepare paraffin sections, blocks of tissue (~3 mm cubes) were fixed in 4% paraformaldehyde for 1 h at room temperature. Following graded dehydration in ethanol, tissue blocks were transferred to xylene and incubated for 10 min with stirring. This step was repeated and tissue blocks were then embedded in paraffin by standard methods. Sectioning to 5–10 µm thickness was performed with a rotary microtome (Leica RM2155). Selected sections were mounted on slides and the paraffin removed by washing twice in xylene (5 min each wash). Xylene was then removed by washing the slides in ethanol twice (5 min each wash), after which a graded rehydration step was conducted in ethanol to phosphate-buffered saline (PBS). The slides were boiled for 20 min in a staining dish in the presence of 100 mM sodium citrate buffer, pH 6.0. After cooling at room temperature for 20 min, the slides were washed twice in PBS for 5 min.

Before hybridization, tissue sections on the slides were incubated with blocking buffer (3% dry milk in PBS, 0.1% Tween-20, and whole goat polyclonal IgG (Santa Cruz

Biotechnology, Santa Cruz, CA, catalog sc-6654) at a 1:30 dilution for 4 h at room temperature.

Primary antibodies were prepared in the same blocking buffer at 1:30 dilution. For dual staining, the two primary antibodies were added at the same time. The slides plus primary antibody were incubated typically for 4 h in a humidified chamber. The AbPOPB antibody signal in mature mushrooms was consistently weaker than in immature mushrooms. Therefore, tissue sections were incubated with anti-AbPOPB and anti-amanitin antibodies for 15 hr instead of the usual 4 h. The slides were then rinsed twice for 5 min each time in PBS buffer and incubated with secondary antibody, diluted according to the manufacturer's instructions in blocking buffer, in a humidified chamber for 2 h. The slides were rinsed twice for 10 min each in PBS, mounted with one drop of Citifluor (Citifluor Ltd, Leicester, United Kingdom), and viewed with an Olympus FV1000D confocal laser confocal scanning microscope.

The anti-amanitin antibody was obtained from Heinz Faulstich (Heidelberg, Germany) (14). The antibody had been raised in rabbits and purified by affinity chromatography. It can detect 1.5 ng/ml α-amanitin in human serum and urine. It reacts with α- and γ-amanitin but not β-amanitin or phallotoxins (14). Most specimens of *A. bisporigera* produce α-, β-, γ-, and ε-amanitin as well as several phallotoxins (21).

The antibodies against AbPOPA and AbPOPB were raised in mouse (Cocalico Biologicals, Reamstown, PA). Whole serum was used for immunoblots and immunohistology. A monoclonal antibody against a synthetic actin C-terminal peptide was produced in mouse (Sigma-Aldrich A3853). The secondary antibodies used were

Alexa Fluor 488 goat anti-mouse IgG (Invitrogen A11029) and Alexa Fluor 594 goat anti-rabbit IgG (Invitrogen A11037).

The specificity of the antibody was tested by immunoblotting against inclusion bodies of *Escherichia coli* expressing AbPOPB and against total extracts of *A. bisporigera*. Total protein was obtained by grinding 0.5 g frozen basidiocarps of *A. bisporigera* in liquid nitrogen. To the resulting powder was added 2 ml of a stock solution of protease inhibitors. The stock solution was made by dissolving five tablets of Complete Mini EDTA-free Protease Inhibitor (Roche Applied Science, Mannheim, Germany) in 5 ml water and adding an additional 5 ml of Protease Inhibitor Cocktail (Sigma P2714) diluted with water according to the manufacturer's instructions. The homogenate was centrifuged at 14,000 × *g* in 1.5-ml microtubes for 15 min. The supernatant was fractionated by SDS-PAGE (pre-made gels of 7.5% acrylamide in Tris-HCl, Bio-Rad, Richmond, CA). The SDS-PAGE markers were Bio-Rad Precision Plus (Dual Color). In order to minimize proteolytic degradation of the POP proteins, the entire extraction procedure was performed in less than 30 min and all solutions were kept on ice or at 4°C. Proteins were transferred to nitrocellulose membrane (Bio-Rad, catalog 162-0115) and detected using ECL Western Blotting Substrate according to the manufacturer's instructions (Pierce, Rockford, IL, catalog 32106). Anti-POP antiserum was incubated with the membrane for 30 min. The membranes were subsequently exposed on Hyperfilm MP (Amersham/GE Healthcare, Buckinghamshire, United Kingdom) for 15 to 60 sec.

Isolation and expression of prolyl oligopeptidase genes. For cloning *AbPOPA* and *AbPOPB*, PCR primers corresponding to the N- and C-termini of both putative genes

(forward primers: 5'-GAAACGAGAGGCGAAGTCAAGGTG-3' and 5'-TCAAATGAAGTAGACGAATGGAC-3'; reverse primers: 5'-AAGTGGATGACGATTATGCGGCAG-3' and 5'-CACACGGATGAGCAATGGATGAG-3') were used in both combinations and the amplicons cloned into *E. coli* DH5α. These primers were based on the partial genomic sequence of *A. bisporigera* (10). The amplicons were cloned into *E. coli* DH5α and sequenced. The full sequences of the genes were obtained from lambda clones (see below). Full-length cDNA copies were obtained by 5' and 3' Rapid Amplification of cDNA Ends (RACE) (18) using primers 5'-ATGTCTCGCCGAACTCGCCGCCTCCTC-3' (5'-RACE) and 5'-GATTGGGTATTTGGCGCAGAAGTCACG-3' (3'-RACE) for *AbPOPA* and primers 5'-GTGACGAACGATGAACATTGGAACTT-3' and 5'-GAAGATGGTAAATATGTGGCCCTGTA-3' for *AbPOPB*. Sequences generated from the RACE reactions were used to assemble full-length cDNAs of *AbPOPA* and *AbPOPB*.

AbPOPA and *AbPOPB* cDNAs were cloned into the pET21 vector between the *BamH*I and *Not*I sites. T-7 tagged versions of both genes were also generated. The expression constructs were transformed into *E. coli* strain BL21 (DE3) (Novagen, EMD Chemicals, Inc., Darmstadt, Germany) and three positive clones for each construct were selected. Expression was induced in a 50-ml culture at an OD_{600} of 0.7 with 0.4 mM isopropyl β-D-1-thiogalactopyranoside (IPTG) following the manufacturer's protocols (Novagen, 11th edition). The cells were disrupted by freeze/thaw treatment and treated with 0.5 U/ml Benzonase nuclease.

Both expressed POP proteins were present in inclusion bodies and yielded no detectable activity with the chromogenic POP substrate Z-Gly-Pro-pNA (Sigma-Aldrich)

at 1 mM (18). Instead, we purified the inclusion bodies of expressed AbPOPA and AbPOPB. The untagged POP proteins were then separated by SDS-PAGE and gel slices containing the POP proteins were used for antibody production. Anti-AbPOPA antibody was raised in chicken and anti-AbPOPB antibody was raised in mouse by Cocalico Biologicals (Reamstown, PA) using their standard protocols.

Nucleic acid manipulations. DNA for blotting was digested with *Pst*I and electrophoresed in 0.7% agarose. Hybridizations were performed overnight at 65°C in 4x SET, 0.1% sodium pyrophosphate, 0.2% SDS, 10% dextran sulfate, and 625 µg/ml heparin. SET (20×) is 3 M NaCl, 0.6 M Tris, and 0.04 M EDTA, pH 7.4. Full-length cDNAs of *AbPOPA* and *AbPOPB* were labeled with [^{32}P]dCTP to use as probes. To construct the genomic lambda library, genomic DNA of *A. bisporigera* was partially digested with *Bfuc*I and electrophoresed in a 0.5% agarose gel at 5 V/cm. DNA fragments of 12 to 20 kb were recovered with the QIAEX II gel extraction kit (Qiagen, Valencia, CA, catalog 20021). The fragments were cloned into the λBlueSTAR Vector (Novagen). The resulting library was screened with *AbPOPA* and *AbPOPB* cDNA probes by standard methods (28). Positive clones were subcloned into *E. coli* strain BMC25.8 and sequenced.

Nucleotide sequence accession numbers. Sequence data from this article can be found in the GenBank/EMBL database under the following accession numbers: HQ225840 for *AbPOPA*, HQ225841 for *AbPOPB*, and EU196153 (updated) for *MSD-10* of *A. bisporigera*.

RESULTS

Immunolocalization of Amanitin. In order to investigate the types of tissue in which amanitin is distributed within a basidiocarp, samples were examined from several representative tissue types, including pileus (cap), lamella (gill), stipe (stem), and universal veil (Fig. 1). Multiple basidiocarps of different developmental stages and various locations were examined.

The most intense and specific anti-amanitin signals were found in a sub-set of cells located in the hymenium, i.e., on the lamella edges where the basidia are formed (Fig. 2A – C). In some samples, there was a strong signal from the sub-hymenial layer in addition to the cells of the hymenium (Fig. 2D). Under higher magnification of a single lamella, the presence of amanitin in only certain hymenial cells and in the sub-hymenium was clear (Fig. 2E, G). Some of the hymenial cells containing amanitin were true basidia (arrows) because they have sterigmata (the slender projections on the basidia to which basidiospores are attached before they are released) whereas others might be either sterile cells or basidia at different stages of maturity (arrowheads) (Fig. 2E–I). Not all basidia contained amanitin, nor did all sterile cells. Fig. 2I shows hymenial cells in which two basidia with sterigmata did not show the presence of amanitin, whereas several adjacent sterile cells did. The trama (inner part of the lamella) consistently showed weaker staining than the hymenium or the sub-hymenium (Fig. 2A, B, D).

The pileus (cap) of *A. bisporigera* also gave strong signals with the anti-amanitin antibody. Figure 3A shows a cross-section of the pileus of a young specimen of *A. bisporigera* and Fig. 3B shows a mature pileus. The individual areas of signal were irregular in shape and their locations did not correspond to cellular boundaries (Fig. 2B, C). The areas giving amanitin signal were consistently smaller than the cells. In Fig. 3C,

the cellular boundaries of the section in Fig. 3B have been outlined in white in order to better illustrate this point. The apparent subcellular localization of amanitin was also visible at higher magnification, where the outlines of individual cells could be seen (Fig. 3D). A similar irregular and apparent subcellular pattern of amanitin distribution was seen in the stipe (Fig. 3E) and in the universal veil (Fig. 3F).

Mushrooms of the amanitin-nonproducing species *A. citrina* and *A. muscaria* were fixed, sectioned, and treated identically with the anti-amanitin antibody. No signals were seen in any sections (data not shown).

In order to improve visualization of background cells not containing amanitin, a universal anti-actin antibody was used as a general indicator of all cells. Figures 4A–C show immunostaining of lamellae with anti-amanitin antibody, anti-actin antibody, and a merge of the two. Figures 4D–F show higher magnification of a single lamella. Amanitin was present in the trama, the subhymenium, and a subset of cells in the hymenium (Fig. 4C, F). Compared to amanitin distribution, the anti-actin antibody produced an even staining throughout the lamellae, as expected for the distribution of a housekeeping protein, with a somewhat stronger signal in the hymenium (Fig. 4B, E).

Identification of a candidate amatoxin-processing peptidase in *A. bisporigera*. It is of particular interest to understand the relationship between the sites of amanitin accumulation and amanitin biosynthesis. To date, no enzymes involved in amatoxin biosynthesis except those coding the toxins themselves have been identified (10, 18). A prolyl oligopeptidase (POP) from the phalloidin-producing mushroom *Conocybe apala* cleaves a synthetic phalloidin proprotein to release the linear heptapeptide corresponding to mature phalloidin, consistent with this enzyme being responsible for the initial

cleavage of the toxin propeptides (18). Using the *C. apala* POP protein (GenBank ACQ65797) and the human POP protein (BAA86936) as queries, we identified partial sequences for two POP genes, *AbPOPA* and *AbPOPB*, in the genome survey sequence of *A. bisporigera*. Based on an analysis of a partial genome sequence of *Galerina marginata*, which makes amatoxins (but not phallotoxins), this mushroom also has two POP genes (22, and our unpublished results). In contrast, all other basidiomycetes whose full genomes were available in GenBank or at the DOE Joint Genome Institute as of May, 2010, have a single POP gene (10). Highly similar orthologs of *AbPOPA* and *AbPOPB* are present in plants, bacteria, and animals. No evidence was found for any POP genes in ascomycetes, except perhaps weakly similar orthologs in *Nectria haematococca* (EEU39197) and *Phaeosphaeria nodorum* (XP_001801532).

The two predicted POP genes of *A. bisporigera* and their corresponding cDNA copies were cloned and sequenced. *AbPOPA* and *AbPOPB* each have 18 introns (Fig. 5). The amino acid sequences of the predicted translational products of *AbPOPA* (761 amino acids) and *AbPOPB* (730 amino acids) were 57% identical to each other and 62% and 57% identical, respectively, to the phalloidin-processing POP (733 amino acids) of *C. apala* (18).

Within the genus *Amanita*, the genes encoding α-amanitin and phallacidin (*AMA1* and *PHA1*, respectively) were found by DNA blotting to be present only in species that make these compounds (10). We probed genomic DNA blots of 13 species in the genus *Amanita*, representing all five sections, with *AbPOPA* and *AbPOPB*. DNA from all of the tested species showed hybridization to a *AbPOPA* probe, whereas only DNA from species in section *Phalloideae*, which contains all of the amatoxin- and phallotoxin-

producing species, showed hybridization to an *AbPOPB* probe (Fig. 6). Due to taxonomic divergence and variation in loading, some of the signals with *AbPOPA* were weak (Fig. 6A). However, most significantly, DNA from none of the species in section *Validae*, the sister group to section *Phalloideae*, showed hybridization to *AbPOPB* even with prolonged exposure (Fig. 6A, lanes 5 – 8). DNA from these same specimens showed the same pattern of hybridization or nonhybridization with *AMA1* and *PHA1* probes (10).

Because the genes of a particular secondary metabolite biosynthetic pathway tend to be clustered in fungi, clustering of *AbPOPA* or *AbPOPB* with other genes involved in amatoxin biosynthesis would suggest a role for one or both of these genes in amatoxin biosynthesis (1, 27, 35). To test this, we screened a lambda phage clone library with *AbPOPA* and *AbPOPB*, and two hybridizing clones were sequenced completely. FGENESH (www.softberry.com) was used to predict proteins *ab initio* using the *Coprinopsis cinerea* model. Each predicted protein was then used to search GenBank nr using BLASTP. Five genes were predicted in the 13.5-kb *AbPOPA*-containing clone (Fig. 7). Gene 4 was *AbPOPA*. The predicted products of genes 1, 2, 3, and 5 had strong hits (score < 1e-62) to hypothetical proteins in other basidiomycetes. Genes 3 and 5 were predicted to encode mitochondrial transporters (pfam 00153) with orthologs in other basidiomycetes.

Six genes were predicted by FGENESH in the 16.0-kb lambda clone containing *AbPOPB*. None had expect scores less than 1e-26 against any protein in GenBank nr. The best hits of genes a, c, e, and f were to hypothetical proteins in the ectomycorrhizal basidiomycete *Laccaria bicolor*. Gene b was *AbPOPB*. Gene d was a member of the MSDIN family previously identified in the genome survey sequence of *A. bisporigera*

(*MSD-10*; GenBank EU196153). A full-length cDNA copy of *MSD-10* was obtained using 5' and 3' RACE, indicating that this gene is expressed and contains three introns, like *AMA1* and *PHA1*. The predicted amino acid sequence of the hypervariable putative toxin region of MSD-10 is GAYPPVPMP, and therefore *MSD-10* is predicted to encode a cyclic nonapeptide containing four Pro residues and lacking tryptathionine.

Immunolocalization of *A. bisporigera* prolyl oligopeptidase B. Based on these several lines of evidence supporting a role for AbPOPB in the biosynthesis of amatoxins in *A. bisporigera*, antibodies were raised against AbPOPB in order to determine the relationship between cellular amatoxin accumulation and biosynthesis. Because neither *AbPOPA* nor *AbPOPB* could be expressed in an enzymatically active form in either *E. coli* or *Pichia pastoris* (unpublished results), we isolated AbPOPB from inclusion bodies of *E. coli* (Fig. 8). The resulting anti-AbPOPB antibody did not recognize other proteins in total extracts of *A. bisporigera* (Fig. 8). Like other fungal POPs (18), AbPOPB was very sensitive to degradation during extraction. Full-length AbPOPB could not be detected without the addition of high levels of protease inhibitors in the extraction buffer. Even then, degradation usually occurred, as could be seen at high protein loadings (Fig. 8). Although antibodies against AbPOPA were successfully raised, the antibodies failed to produce a clear and specific signal when tested on whole mushroom extracts (data not shown). We therefore used only the anti-AbPOPB antibody for immunohistochemical studies.

Dual labeling of pileus (cap) tissue from an immature mushroom indicated strong co-localization of amanitin and AbPOPB, as indicated by the orange to yellow color (Fig. 9). Figures 9D – F show higher magnification views of the area indicated by the white box in

Fig. 9C. Calculation of the overlap coefficients showed 52.0% of AbPOPB co-localizing with amanitin and 99.9% of amanitin co-localizing with AbPOPB. Co-localization of amanitin and AbPOPB were also examined in lamellae (Fig. 9G – I). The merge between the two (i.e., orange to yellow color) showed significant overlap of the two signals (Fig. 9I). Amanitin and AbPOPB were both present in certain hymenial cells and not others (Fig. 9G – I). Several areas were analyzed and the co-localization was calculated at better than 75%.

DISCUSSION

Although amanitins have been known to be distributed throughout the tissue of *Amanita* mushrooms, their cellular localization has not previously been determined (8). Here we show that the distribution of amanitin is not uniform among cells of the basidiocarp, nor are they sequestered in a morphologically distinct cell type, unlike the anti-collembola toxins of *R. bella* or the anti-nematode compounds of *C. apala* (12, 23). Selective distribution of amatoxins was particularly apparent in the organized cells of the hymenium and sub-hymenium as opposed to the interwoven ground hyphae of the pileus and stipe. Furthermore, our results indicate that amanitin is not evenly distributed within the cells. Rather, amanitin appears to be compartmentalized at the sub-cellular level. Although we did not resolve the structures containing amanitin, they are most likely vacuoles, such as are known to be the sites of accumulation of secondary metabolites in other organisms (16). Aflatoxins and some their biosynthetic intermediates accumulate in vacuoles and vesicles in *Aspergillus parasiticus*, even though other steps in aflatoxin biosynthesis occur in peroxisomes or the cytoplasm (26). However, a fundamental

difference between amanitins and aflatoxins (and most other ascomycete secondary metabolites) is that whereas aflatoxins are ultimately secreted into the medium, amanitins are not secreted and are therefore stored inside cells in a way that sequesters them from primary metabolism (37).

A particular question that this paper begins to address is the relationship between amanitin accumulation and amanitin biosynthesis. At this point we know little about the enzymology of the post-translational processing steps of amanitin biosynthesis, which include cleavage of the proprotein, cyclization, hydroxylation, formation of the cross-bridge between Trp and Cys, and, in the case of the phallotoxins, epimerization of L-Thr or L-Asp to the corresponding D isomer.

Several lines of evidence implicate prolyl oligopeptidase (POP) in cleavage of the proprotein, which is the predicted first step of post-translational maturation of the amatoxins and phallotoxins (18). First, all members of the MSDIN family, which includes the genes encoding α-amanitin, β-amanitin, phallacidin, phalloidin, and a cyclic decapeptide related to antamanide, have invariant Pro residues as the amino acid immediately upstream of the hypervariable toxin region that contains the peptide sequence of the mature toxins and as the last amino acid in the toxin region (10, 18, 36). This indicates that posttranslational cleavage of the toxin proproteins is probably catalyzed by a Pro-specific peptidase (6, 29). Second, an enzyme capable of cleaving a phalloidin precursor protein at both Pro residues, resulting in release of the cognate linear heptapeptide, was identified as a POP in the phalloidin-producing mushroom *C. apala* (18).

In this paper we provide additional evidence to support the *in vivo* role of POP in amanitin biosynthesis. First, *AbPOPB*, but not *AbPOPA*, is restricted taxonomically to those species in the genus *Amanita* that make amatoxins. A plausible explanation for why toxic *Amanita* species (and the amanitin-producing species *Galerina marginata*; our unpublished data) have two POP genes whereas other basidiomycetes have only one is that one of the POPs (AbPOPA in the case of *A. bisporigera*) is a housekeeping POP that is functionally equivalent to the single POP found in other basidiomycetes, whereas the second POP (AbPOPB) has a dedicated function in toxin biosynthesis. Although POPs are widespread in nature, having been described in plants, animals, trypanosomes, bacteria, and other basidiomycetes, little is known about their native substrates except in mammals (2). Human POP cleaves several peptide hormones *in vitro* and *in vivo* and has been implicated in human pathologies including dementia, amnesia, multiple sclerosis, and sleeping sickness (24). The native substrates of POPs in other organisms have been little studied. Our results point to the proproteins of the MSDIN family as the probable *in vivo* substrates of a particular class of POPs in certain basidiomycetes.

A third line of evidence in support of a role of AbPOPB in amatoxin processing is genetic linkage between *AbPOPB* and an expressed member of the MSDIN family (*MSD-10*). Clustering of genes involved in a common pathway is the usual situation in fungal secondary metabolism (31). Although there has been less work done on the genetics of secondary metabolism in basidiomycetes compared to ascomycetes, this appears to be the emerging consensus for this group of organisms as well (1, 27, 35).

Taken together, the evidence strongly implicates AbPOPB in the biosynthesis of the amatoxins and phallotoxins, and therefore we raised antibodies against AbPOPB to use as

a marker to localize the site of amanitin biosynthesis. In fact, there was a high degree of co-localization between amanitin and AbPOPB, which is consistent with synthesis and accumulation occurring in the same cells.

Natural products serve as the major source of pharmaceutical agents against a wide variety of old and emerging human diseases. However, most of our medicines are based on only a few fundamental molecular scaffolds, which have been heavily exploited by generations of tailoring (33). Historically, toxins have shown great value in drug development and pharmaceutical use, especially the highly potent ones that have specific targets. *Amanita* toxins are highly potent and highly specific, which has led to their widespread use as research reagents. In several ways, the peptide toxins of *Amanita* are chemically and biochemically unique among known natural products, e.g., they are the only ones that contain the Cys-Trp cross-bridge (tryptathionine), and they are the smallest known ribosomally synthesized peptides. They may therefore provide a novel scaffold on which to design new pharmaceutical agents (9, 19, 20, 25). Identification of the genes and enzymes involved in the biosynthesis of the *Amanita* toxins may make it possible to produce a large number of new compounds based on the naturally occurring toxins.

Compared to the other main groups of micro-organisms that make secondary metabolites (namely, bacteria and ascomycetes), relatively little is known about the chemistry, biochemistry, or biology of secondary metabolites made by higher basidiomycetes, commonly known as mushrooms (27). Compared to ascomycetes and bacteria, mushrooms have more complex anatomies and consequently more cell specialization. The results presented in this paper illustrate this cellular specialization for both toxin accumulation and biosynthesis.

ACKNOWLEDGMENTS

We thank Heniz Faulstich (Heidelberg, Germany) for the generous gift of anti-amanitin antibodies, Melinda Frame of the Michigan State University (MSU) Microscopy Facility and Markus Günl (MSU) for scientific advice, and Federica Brandizzi (MSU) for comments on the manuscript. This work was funded by grant DE-FG02-91ER200021 from the U.S. Department of Energy Office of Basic Energy Sciences, Division of Chemical Sciences, Geosciences and Biosciences.

REFERENCES

1. **Agger, S., F. Lopez-Gallego, and C. Schmidt-Dannert.** 2009. Diversity of sesquiterpene synthases in the basidiomycete *Coprinus cinereus*. Mol. Microbiol. **72:**1181–1195.
2. **Bastos, I. M., F. N. Motta, S. Charneau, J. M. Santana, L. Dubost, K. Augustyns, and P. Grellier.** 2010. Prolyl oligopeptidase of *Trypanosoma brucei* hydrolyzes native collagen, peptide hormones and is active in the plasma of infected mice. Microbes Infect. **12**:457–466.
3. **Bresinsky, A., and H. Besl.** 1990. *In* A Colour Atlas of Poisonous Fungi: A Handbook for Pharmacists, Doctors and Biologists. Wolfe, Würzburg, Germany.
4. **Bushnell, D. A., P. Cramer, and R. D. Kornberg.** 2002. Structural basis of transcription: alpha-amanitin-RNA polymerase II cocrystal at 2.8 A resolution. Proc. Natl. Acad. Sci. USA **99:**1218–1222.

5. **Clémençon, H.** 2004. *In* Cytology and Plectology of the Hymenomycetes. J. Cramer, Berlin.
6. **Cunningham, D. F., and B. O'Connor.** 1997. Proline specific peptidases. Biochim. Biophys. Acta **1343:**160–186.
7. **Enjalbert, F., C. Gallion, F. Jehl, H. Monteil, and H. Faulstich.** 1992. Simultaneous assay for amatoxins and phallotoxins in *Amanita phalloides* Fr. by high-performance liquid chromatography. J. Chromatogr. **598:**227–236.
8. **Enjalbert, F., G. Cassanas, S. L. Salhi, C. Guinchard, and J. -P. Chaumont.** 1999. Distribution of the amatoxins and phallotoxins in *Amanita phalloides*. Influence of the tissues and the collection site. C.R. Acad. Sci. III **322:**855–862.
9. **Fischbach, M. A., and C. T. Walsh.** 2009. Antibiotics for emerging pathogens. Science **325:**1089–1093.
10. **Hallen, H. E., H. Luo, J. S. Scott-Craig, and J. D. Walton.** 2007. Gene family encoding the major toxins of lethal *Amanita* mushrooms. Proc. Natl. Acad. Sci. USA **104:**19097–19101.
11. **Hallen, H. E., R. Watling, and G. C. Adams.** 2003. Taxonomy and toxicity of *Conocybe lactea* and related species. Mycol. Res. **107:**969–979.
12. **Hutchison, L. J., S. E. Madzia, and G. L. Barron.** 1996. The presence and antifeedant function of toxin-producing secretory cells on hyphae of the lawn-inhabiting agaric *Conocybe lactea*. Can. J. Bot. **74:**431–434.
13. **Jenkinson, T. S., G. J. Celio, M. Padamsee, B. T. M. Dentinger, M. L. Meyer, and D. J. McLaughlin.** 2008. Conservation of cytoplasmic organization in the cystidia of *Suillus* species. Mycologia **100:**539–547.

14. **Kirchner, K., and H. Faulstich.** 1986. Purification of amatoxin-specific antibodies from rabbit sera by affinity chromatography, their characterization and use in toxicological studies. Toxicon **24**: 273–283.

15. **Kuo, M.** 2006. Using a microscope: Basidia and cystidia. http://www.mushroomexpert.com/microscope_cystidia.html.

16. **Kutchan, T. M.** 2005. A role for intra- and intercellular translocation in natural product biosynthesis. Curr. Opin. Plant Biol. **8:**292–300.

17. **Largent, D. L., and D. Johnson.** 1977. *In* How to Identify Mushrooms to Genus III: Microscopic Features. Mad River Press, Eureka, California.

18. **Luo, H., H. E. Hallen-Adams, and J. D. Walton.** 2009. Processing of the phalloidin proprotein by prolyl oligopeptidase from the mushroom *Conocybe albipes*. J. Bio. Chem. **284:**18070–18077.

19. **May, J. P., and D. M. Perrin.** 2007. Tryptathionine bridges in peptide synthesis. Pept. Sci. **88:**714–724.

20. **McIntosh, J. A., Donia, M. S., and E. W. Schmidt.** 2009. Ribosomal peptide natural products: bridging the ribosomal and nonribosomal worlds Nat. Prod. Rep. **26:**537–559.

21. **McKnight, T. A., K. B. McKnight, and M. C. Skeels.** 2010. Amatoxin and phallotoxin concentration in *Amanita bisporigera* spores. Mycologia **102**:763-5.

22. **Nagendran, S., H. E. Hallen-Adams, J. M. Paper, N. Aslam, and J. D. Walton.** 2009. Reduced genomic potential for secreted plant cell-wall-degrading enzymes in the ectomycorrhizal fungus *Amanita bisporigera*, based on the secretome of *Trichoderma reesei*. Fung. Genet. Biol. **46:**427–435.

23. **Nakamori, T, and A. Suzuki.** 2007. Defensive role of cystidia against Collembola in thebasidiomycetes *Russula bella* and *Strobilurus ohshimae*. Mycol. Res. **111:**1345–1351.

24. **Nolte, W. M., D. M. Tagore, W. S. Lane, and A. Saghatelian.** 2009. Peptidomics of prolyl endopeptidase in the central nervous system. Biochemistry **48**:11971–11981.

25. **Oman, T. J., and W. A. van der Donk.** 2010. Follow the leader: the use of leader peptides to guide natural product biosynthesis. Nat. Chem. Biol. **6:**9–18.

26. **Roze, L. V., A. Chanda, and J. E. Linz.** 2010. Compartmentalization and molecular traffic in secondary metabolism: A new understanding of established cellular processes. Fung. Genet. Biol., in press. doi:10.1016/j.fgb.2010.05.006.

27. **Schneider, P., S. Bouhired, and D. Hoffmeister.** 2008. Characterization of the atromentin biosynthesis genes and enzymes in the homobasidiomycete *Tapinella panuoides*. Fung. Genet. Biol. **45:**1487–1496.

28. **Scott-Craig, J. S., D. G. Panaccione, F. Cervone, and J. D. Walton.** 1990. Endopolygalacturonase is not required for pathogenicity of *Cochliobolus carbonum* on maize. Plant Cell **2:**1191–1200.

29. **Szeltner, Z., and L. Polgár.** 2008. Structure, function and biological relevance of prolyl oligopeptidase. Curr. Protein Pept. Sci. **9:**96–107.

30. **Truong, B. -N., K. Okazaki, T. Fukiharu, Y. Takeuchi, K. Futai, X. -T. Le, and A. Suzuki.** 2007. Characterization of the nematocidal toxocyst in *Pleurotus* subgen. *Coremiopleurotus*. Mycoscience **48:**222–230.

31. **Walton, J. D.** 2000. Horizontal gene transfer and the evolution of secondary metabolite gene clusters in fungi: An hypothesis. Fung. Genet. Biol. **30:**167–171.

32. **Walton, J. D., D. G. Panaccione, and H. E. Hallen.** 2004. Peptide synthesis without ribosomes. *In* J. Tkacz and L. Lange (ed.), Advances in Fungal Biotechnology for Industry, Agriculture, and Medicine, p. 127–162. Kluwer Academic, New York, NY.

33. **Walsh, C. T., and M. A. Fischbach. 2010.** Natural products version 2.0: connecting genes to molecules. J. Am. Chem. Soc. **132:**2469-2493.

34. **Watkins, M., D. R. Hillyard, and, B. M. Olivera.** 2006. Genes expressed in a turrid venom duct: divergence and similarity to conotoxins. J. Mol. Evol. **62:**247–256.

35. **Welzel, K., K. Eisfeld, L. Antelo, T. Anke, and H. Anke.** 2005. Characterization of the ferrichrome A biosynthetic gene cluster in the homobasidiomycete *Omphalotus olearius*. FEMS Microbiol. Lett. **249:**157–163.

36. **Wieland, T.** 1986. *In* A. Rich (ed.), Peptides of Poisonous *Amanita* Mushrooms. Springer, New York, NY.

37. **Zhang, P., Z. Chen, J. Hu, B. Ei, Z. Zhang, and W Hu.** 2005. Production and characterization of amanitin toxins from a pure culture of *Amanita exitialis*. FEMS Microbiol. Lett. **252:**223–228.

FIGURE LEGENDS

FIG. 1. (A) Mature basidiocarps of *Amanita bisporigera* used in this study (collected in Ingham County, Michigan, in August, 2009). (B) Immature basidiocarps collected before emergence from the ground. Intact basidiocarps are shown on the right, and longitudinal sections through the same basidiocarps on the left. Structures: a, pileus (cap); b, stipe (stem); c, universal veil, giving rise to the volva at the base of the stem as indicated in (A); d, lamella (gill).

FIG. 2. Amanitin immunostaining of lamellae (gills) of *A. bisporigera* observed by confocal laser scanning microscopy (CLSM). (A) Low-magnification CLSM view showing cross-section of two lamellae and part of a third. (B) Higher magnification of a single lamella by CLSM. (C) Same gill section as in (B) viewed by differential interference contrast (DIC). (D) A different basidiocarp showing a cross-section of three lamellae and parts of two others by CLSM. (E) Anti-amanitin immunostaining of basidia (arrows), indicated by the sterigmata (the two slender projections), sterile cells (arrow heads), and the sub-hymenium (CLSM superimposed on DIC). Sterigmata are the slender projections from the basidia that bear the basidiospores, which are no longer present in these sections. Sterile cells are the cells in the hymenium that, in *Amanita*, resemble basidia but do not bear spores. (F) Same section as in (E) viewed with DIC alone. (G) Anti-amanitin immunostaining of hymenium and sub-hymenium showing basidia (arrows) with sterigmata and sterile cells containing amanitin (CLSM superimposed on DIC). (H) Same section as in (G) observed by DIC. (I) Basidia (arrows) showing absence of

amanitin and adjacent sterile cells (arrow heads) showing presence of amanitin (CLSM superimposed on DIC).

FIG. 3. Amanitin immunostaining of different tissues of *A. bisporigera* by LSM. (A) Section of the pileus of the immature basidiocarp shown in Fig. 1B. (B) Section of a mature pileus. (C) Same view as in (B) with white lines manually drawn to highlight outlines and boundaries of the cells. (D) Higher magnification of an individual hypha of a mature pileus (CLSM superimposed on DIC). (E) Section of stipe (stem) of a mature basidiocarp. (F) Section of a universal veil (volva) of a mature basidiocarp (see Fig. 1A).

FIG. 4. Dual immunostaining of *A. bisporigera* lamellae using anti-amanitin and anti-actin antibodies. (A – C) Lamella cross-sections: left to right show amanitin staining, actin staining and the merge of the two. (D – F) Higher magnification views of a cross-section of a lamella (same staining order as above). (G – H) Higher magnification views of a cross-section of a mature pileus.

FIG. 5. Gene structure of *AbPOPA* and *AbPOPB* of *A. bisporigera*.

FIG. 6. DNA blotting of 13 *Amanita* species probed with (A) *AbPOPA* or (B) *AbPOPB*. The species are: Lane 1, *A.* aff. *subalbiacea*; lane 2, *A. bisporigera*; lane 3, *A. phalloides*; lane 4, *A. ocreata*; lane 5, *A. novinupta*; lane 6, *A. flavoconia*; lane 7, A. *porphyria*; lane 8, *A. franchetii*; lane 9, *A. muscaria*; lane 10, *A. gemmata*; lane 11, *A. hemibapha*; lane 12, *A. velosa*; lane 13, unidentified species of *Amanita* sect. *Vaginatae*.

Mushrooms represent sections *Phalloideae* (1–4), *Validae* (5–8), *Amanita* (9 and 10), *Caesareae* (11), and *Vaginatae* (12 and 13). Approximately the same amount of DNA was loaded in each lane (see reference 10).

FIG. 7. Gene maps of lambda phage clones containing (A) *AbPOPA* or (B) *AbPOPB*. Arrows indicate transcriptional direction. Genes were predicted using FGENESH (www.softberry.com).

FIG. 8. Immunoblotting of *E. coli* inclusion bodies and total extracts of *A. bisporigera* with anti-AbPOPB antibody. Lanes: 1, BL21 empty vector (PET21) control; 2, inclusion body (1 µl = 0.05 µg) of an *E. coli* BL21 line expressing AbPOPB; Lanes 3 through 6, total soluble protein from *A. bisporigera* loaded at 24 µg, 47 µg, 94 µg and 141 µg, respectively. All lanes were from the same gel, but some lanes between lanes 1 and 2 were removed. Size indicators (left) are in kDa.

FIG. 9. Co-localization of amanitin and AbPOPB. (A – C) Co-localization in the pileus. The stipe is on the left. From left to right: anti-amanitin, anti-AbPOPB, and merge of (A) and (B). (D – F) Higher magnification of a portion of the pileus in (A – C). **(G – I)** Co-localization in a single lamella, same order as (A – C).

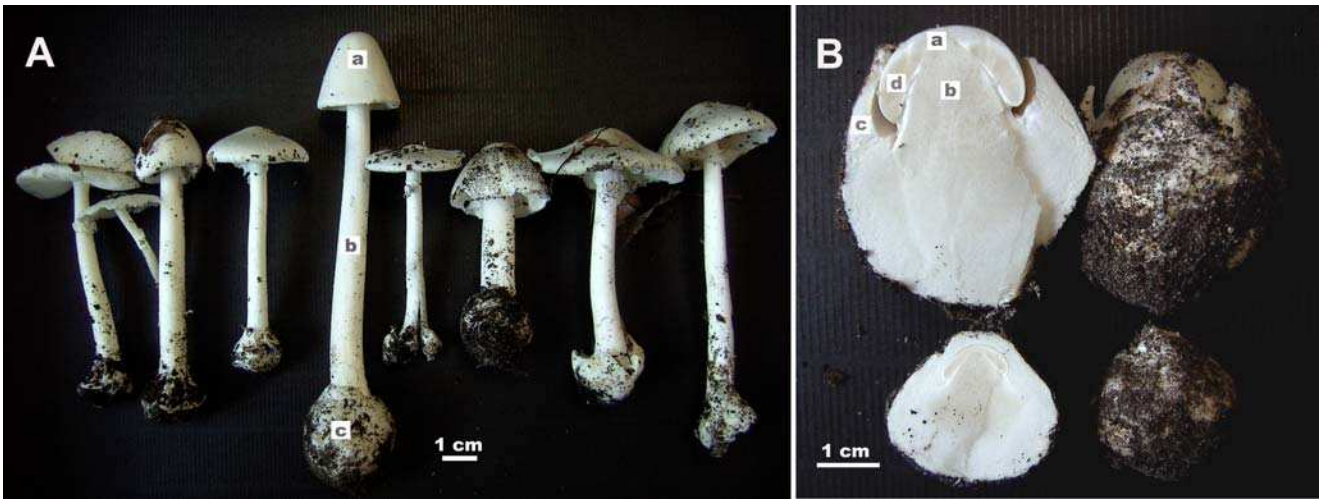

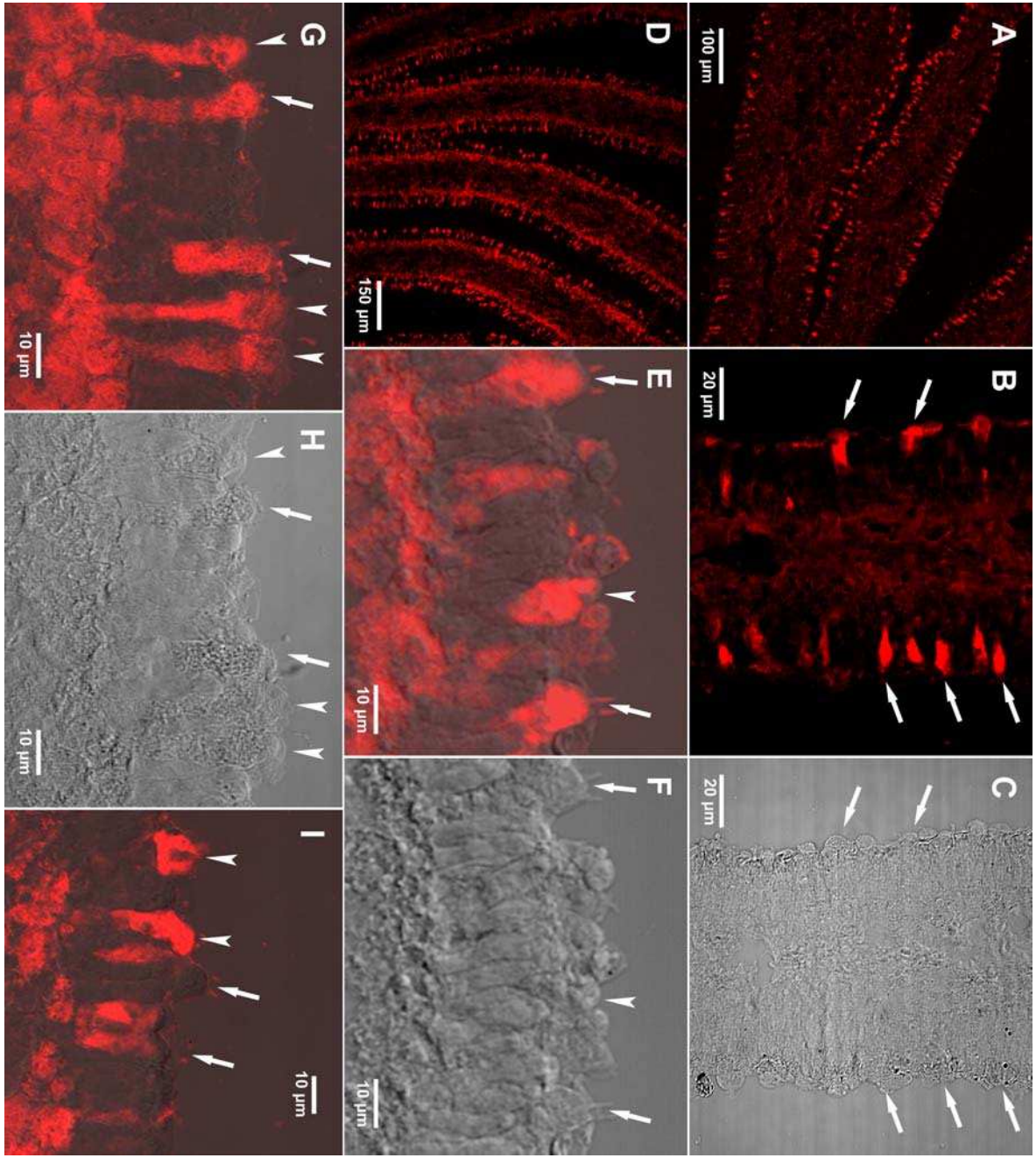
A
100 µm
B
20 µm
C
20 µm
D
150 µm
E
10 µm
F
10 µm
G
10 µm
H
10 µm
I
10 µm

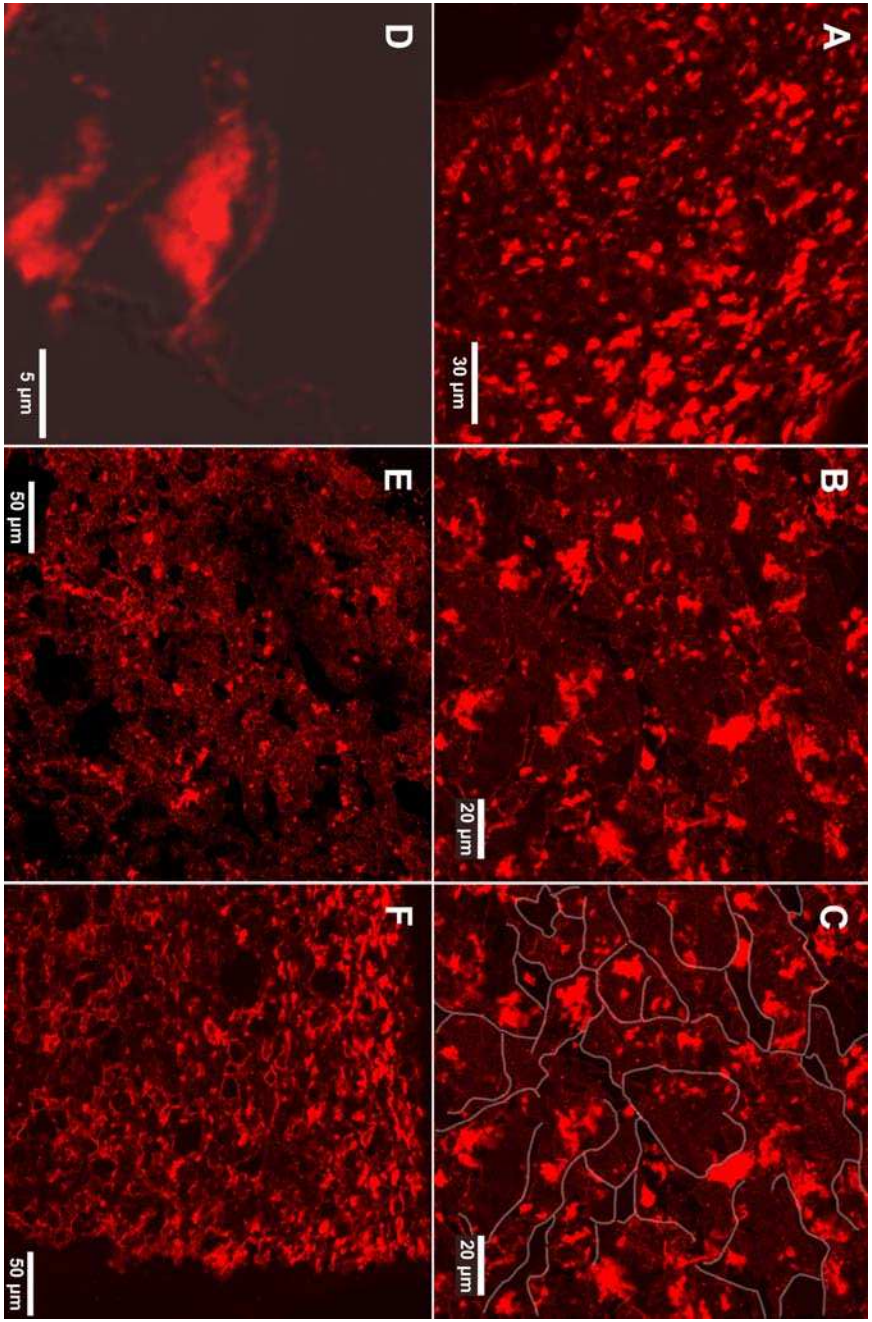
A
30 µm
B
20 µm
C
20 µm
D
5 µm
E
50 µm
F
50 µm

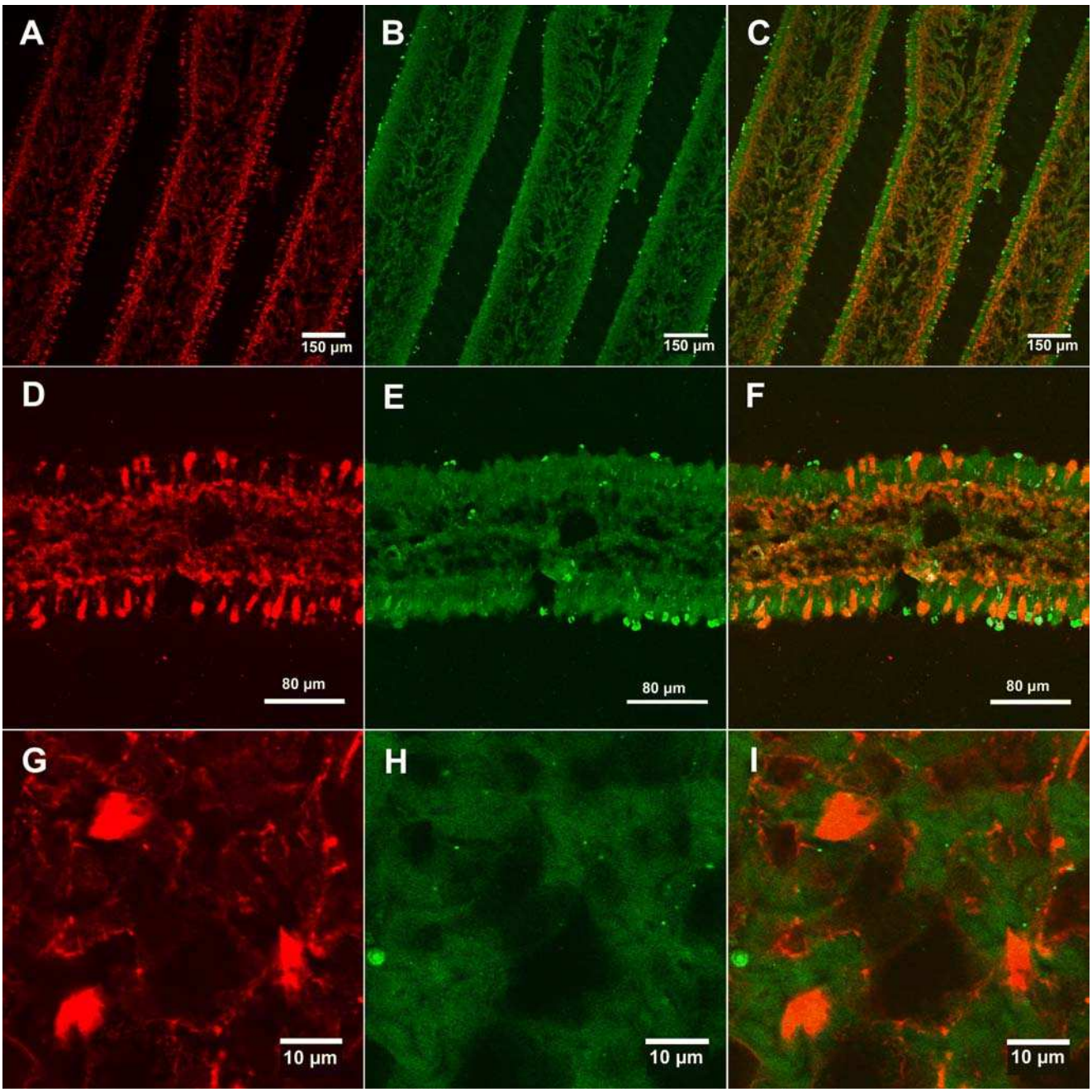

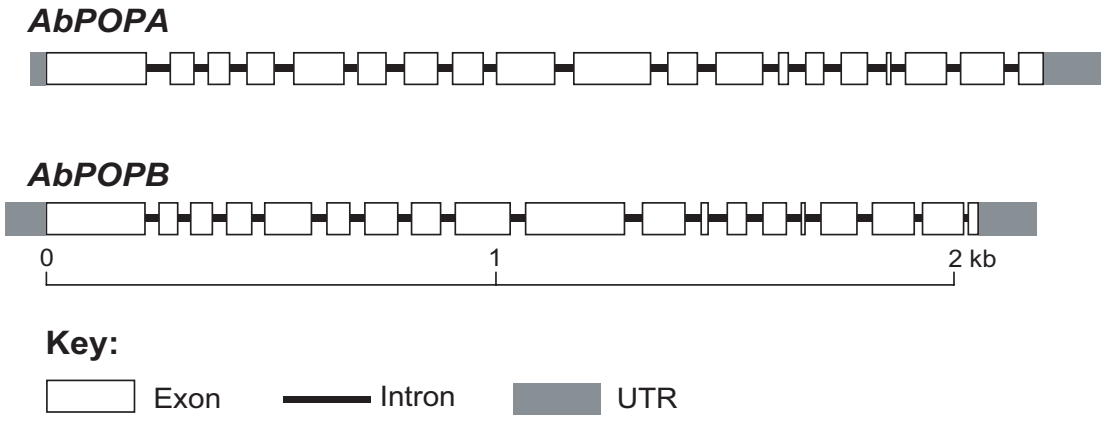

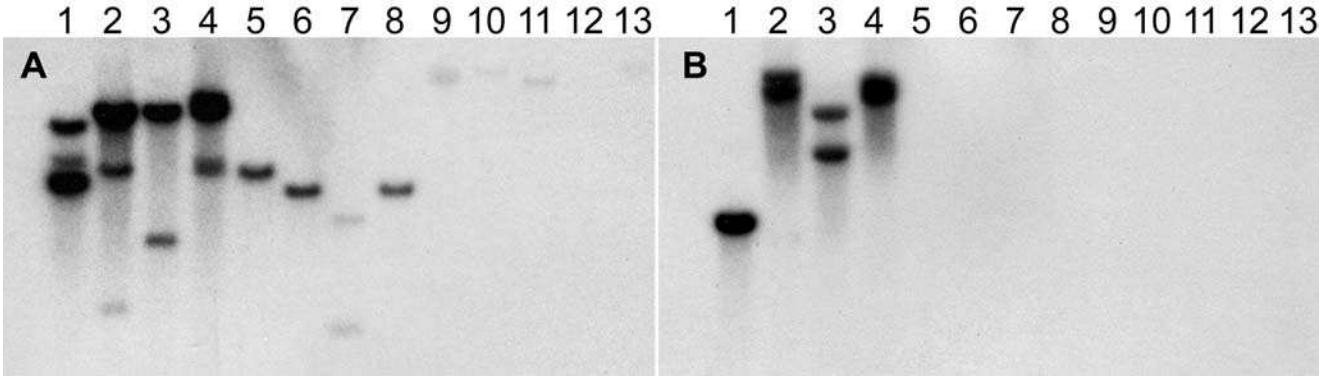

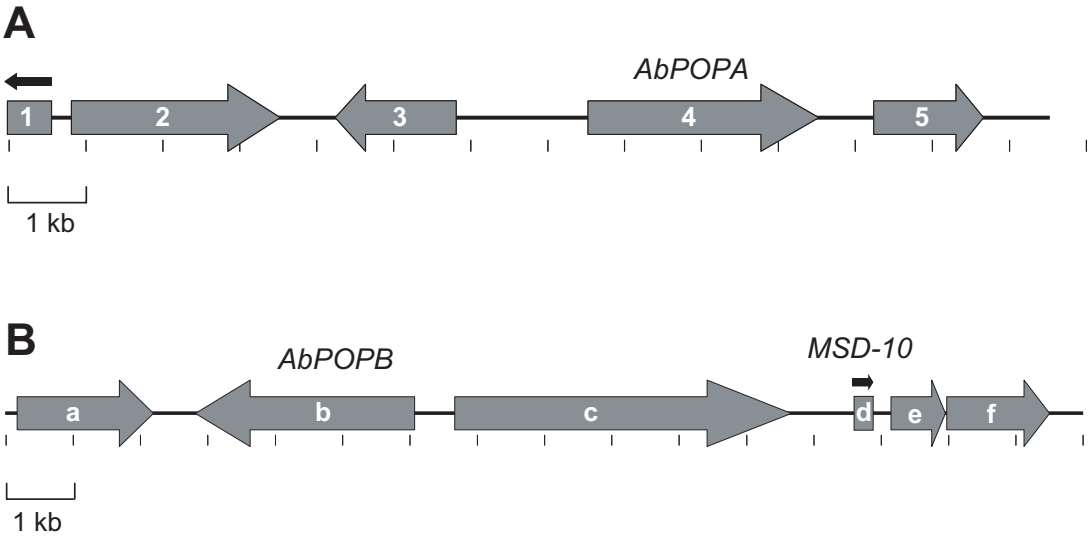

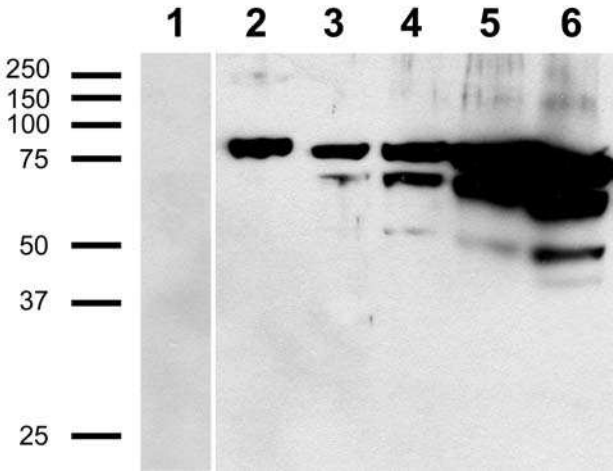

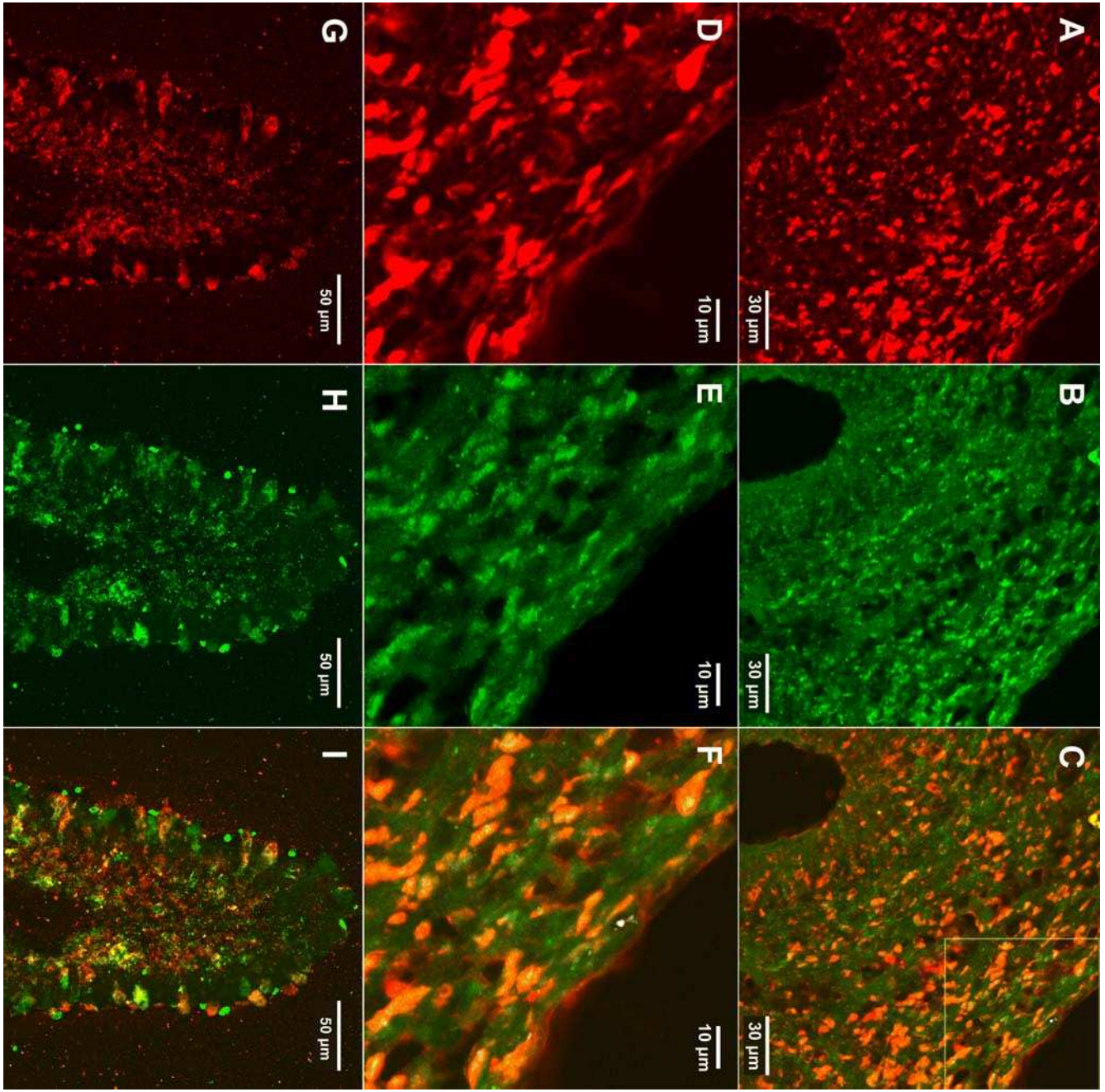
A
30 µm
B
30 µm
C
30 µm
D
10 µm
E
10 µm
F
10 µm
G
50 µm
H
50 µm
I
50 µm